RESEARCH ARTICLE

A sorption kinetics model for arsenic adsorption to magnetite nanoparticles

Heather J. Shipley · Sujin Yean · Amy T. Kan · Mason B. Tomson

Abstract

Introduction Arsenic is a well known water contaminant that causes toxicological and carcinogenic effects. In this work magnetite nanoparticles were examined as possible arsenic sorbents. The objective of this work was to develop a sorption kinetics model, which could be used to predict the amount of arsenic adsorbed by magnetite nanoparticles in the presence of naturally occurring species using a first-order rate equation, modified to include adsorption, described by a Langmuir isotherm.

Discussion Arsenate and arsenite adsorption to magnetite nanoparticles was studied, including the effect of naturally occurring species (sulfate, silica, calcium magnesium, dissolved organic matter, bicarbonate, iron, and phosphate) on adsorption.

Conclusion The model accurately predicts adsorption to magnetite nanoparticles used in a batch process to remove arsenic from spiked Houston, TX tap water, and contaminated Brownsville, TX groundwater.

Keywords Sorption · Arsenic · Nanoparticles · Kinetics

Responsible editor: Elena Maestri

H. J. Shipley (✉)
University of Texas–San Antonio,
One UTSA Circle,
San Antonio, TX 78249, USA
e-mail: heather.shipley@utsa.edu

S. Yean
Integrated Laboratory Technologies, Oilfield Chemistry,
Chevron Energy Technology Company,
3901 Briarpark,
Houston, TX 77042, USA

A. T. Kan · M. B. Tomson
Rice University,
6100 Main Street MS-519,
Houston, TX 77005, USA

1 Introduction

Currently, many methods exist to remove arsenic from potable water, such as coagulation, ion exchange, membrane filtration, and adsorption with iron and aluminum oxides. Arsenic removal methods are needed because millions of people in Southeast Asia and 13 million people in the USA are exposed to arsenic concentrations greater than 10 μg/L in their drinking water (World Health Organization 2001). There are regulatory limits on arsenic in the drinking water because of its known chronic toxicological and carcinogenic effects (black foot, skin, bladder, and lung cancer, still births, and heart attacks; Smedley and Kinniburgh 2002). In January 2006, the USEPA lowered the maximum contaminant level (MCL) from 50 to 10 μg/L (Anderson and Bruland 1991; Frankenberger 2002; Smedley and Kinniburgh 2002). Many countries, including the USA, now face the dilemma of treating their drinking water to achieve regulatory standards.

Many researchers have studied the adsorption of arsenic onto bulk crystalline iron(III) oxides, such as goethite and hematite, as possible sorbents for arsenic removal (Arai et al. 2004; Coker et al. 2006; Cornell and Schwertmann 1996; Gimenez et al. 2007; O'Day et al. 2005; Pierce and Moore 1982; Raven et al. 1998; Waychunas et al. 1995) and to a lesser effect the mixed iron [Fe(II)/(III)] oxide, magnetite (Dixit and Hering 2003; Ohe et al. 2005). Their work shows that iron oxides can adsorb arsenic, especially arsenate, from solution. A limitation to larger particulate

sorbents is their surface area, which can cause less removal in the presence of other species, and in some cases, large quantities (>1 g/L) of the solid is needed to remove arsenic to below MCL, while amorphous colloids produced by adding iron(III) salts are difficult to remove and tend to bind to filters. Using manmade nanoparticles can create an advantage over bulk crystalline iron oxides because of the increased surface area, which allows for more sorption sites for removal (Banfield and Navrotsky 2003; Rusanov 2005). Unlike bulk crystalline iron oxides, amorphous iron oxides have high specific surface areas equal to or greater than most iron oxide nanoparticles, but they are often difficult to separate and can leave iron residuals in the water after treatment (Hering et al. 1997). In this paper, magnetite nanoparticles are used because of their affinity for both arsenate and arsenite, easy separation from solution with low field magnets or filters, and increased adsorption capacity compared to bulk magnetite particles (Yavuz et al. 2006; Yean et al. 2005).

In the literature, there have been several studies on the effect of carbonate, phosphate, and silica (Appelo et al. 2002; Genc and Tjell 2003; Hongshao and Stanforth 2001; Kanel et al. 2005; Meng et al. 2000; Su and Puls 2001a; Violante and Pigna 2002; Waltham and Eick 2002) on arsenic adsorption, while less work has been conducted on the effect of calcium, magnesium, and dissolved organic matter (DOM) (Grafe et al. 2002). The literature shows that carbonate species decrease arsenic adsorption to ferrihydrite and zero valent iron, but bicarbonate less than 1 mM had negligible effects on iron(III) oxides (Appelo et al. 2002; Kanel et al. 2005; Meng et al. 2000; Su and Puls 2001a). Many researchers have studied the effect of high concentrations of phosphate on arsenic adsorption. Arsenic adsorption to iron(III) oxides was shown to decrease in the presences of 0.01–104 mM phosphate (Genc and Tjell 2003; Hongshao and Stanforth 2001; Jain and Loeppert 2000; Su and Puls 2001b; Violante and Pigna 2002). Several studies have shown for silica that as the concentration increases, arsenic adsorption to iron(III) oxides decreases (Genc and Tjell 2003; Meng et al. 2000; Su and Puls 2001b; Waltham and Eick 2002). For the lesser studied DOM, Grafe et al. (2002) found that the DOM, fulvic acid, did not significantly decrease arsenate adsorption, but it did have an effect on arsenite adsorption to ferrihydrite. In the literature, there appears to be little agreement on the effect of sulfate on arsenic adsorption to iron oxides. Some researchers (Jain and Loeppert 2000) have found that sulfate had no influence on arsenic adsorption to ferrihydrite, while others (Vaishya and Gupta 2003) have found that arsenite adsorption decreased on iron(III)-coated sand.

The overall objectives of this work are to present new data on the effect of common aquatic species on arsenic adsorption to magnetite nanoparticles and to develop a model that can be used for treatment design for the remediation of arsenic from drinking water using magnetite nanoparticles. Results from batch arsenic adsorption studies have been used to develop a sorption kinetics model using a modified rate equation that can predict arsenic adsorption to magnetite nanoparticles in natural waters. Adsorption studies with spiked Houston tap water and arsenic contaminated Brownsville, TX groundwater were conducted and results compared to the arsenic adsorption kinetic results predicted by the model.

2 Materials and methods

2.1 Materials

As(III) and As(V) stock solutions were prepared from arsenic(III) oxide (As_2O_3) (Sigma Aldrich) and arsenic(V) oxide hydrate ($As_2O_5 \cdot 3H_2O$) (Sigma Aldrich), respectively, which yielded 500 mg As(III)/L and 500 mg As(V)/L in 0.1 M NaOH with a final measured pH of 10. The stock solutions were prepared every 3 months and refrigerated. During the 3-month period, arsenic speciation was periodically conducted on the As(III) solution to confirm its stability. Speciation was done by passing the solution through anionic ion exchange cartridges (Supelco Bellefonete, PA), where As(V) was retained in the cartridge and As(III) passed through (Yalcin and Le 2001). As(V) was then eluted from the cartridge with 2% nitric acid. The arsenate and arsenite fraction from the speciation were analyzed separately using Perkin Elmer inductively coupled plasma mass spectrometer (ICP-MS). Speciation results showed that at least 95% of the solution was still arsenite, confirming its stability at the end of 3 months.

The experiments were conducted at a pH of 8.00±0.04 buffered with 0.01 M tris(hydroxymethyl)aminomethane (THAM) buffer. The pH adjustment of the solution was accomplished with either 1 N NaOH or 6 N HNO3.

To test the effects of common aquatic components on arsenic removal stock solutions were prepared by adding bicarbonate (0, 0.16, 0.82, 1.64, 4.1, 8.2 mM) as sodium bicarbonate; silica (0, 0.17, 0.42, 0.83, 1.67 mM) as sodium silicate; DOM (0, 5,10, 25 mg/L) as Suwannee River fulvic acid (IHSS); sulfate (0, 0.52, 1.04, 2.6 mM) as sodium sulfate; ferric iron (0, 0.2, 0.5, 1, 1.5, 2, and 5 mg/L) as ferric chloride; ferrous iron (0, 0.2, 0.5, and 1.0 mg/L) as ferrous chloride; calcium and magnesium (0, 0.33 and 1.32 mM hardness) as chloride salts, calcium chloride and magnesium chloride; and phosphate (0, 1, 5, 10 µM) as dibasic sodium phosphate. If not otherwise specified, reagent grade chemicals were purchased from Fisher Scientific.

Water was prepared by reverse osmosis followed by a four stage ion exchange water purification process, consisting of a Barnstead high capacity cation/anion column, two

Barnstead ultrapure ion exchange columns and then a Barnstead organic removal column.

Brownsville, TX groundwater was collected in one gallon polypropylene containers with no headspace. The samples were kept in the dark in a climate controlled environment during transport (18°C) and subsequently stored in a laboratory refrigerator (4°C). Water analyses were done using HACH standard methods for alkalinity, hardness, phosphate, silica, and sulfate (HACH 2007). Metal concentrations were measured using ICP or ICP-MS. The common aquatic components found in the groundwater were in the same concentration ranges tested for the adsorption experiments except calcium and sulfate which had higher concentrations in the Brownsville groundwater.

2.2 Analytical methods

Arsenic concentrations were measured on a Perkin Elmer Elan 9000 ICP-MS having a quadrupole mass spectrometer. The plasma is Ar gas with a nebulizer gas flow of 0.98 L/min, a lens voltage of 6.5 V, and RF power of 1000 W. These operating conditions were chosen after optimization of each parameter and samples were tested in triplicate.

The arsenic standards were prepared by making a 1.0 mg/L standard stock solution (CPI International Peak Performance standard). Then the stock solution was diluted to the desired calibration standard concentrations of 0, 1, 10, and 100 µg/L. The calibration standards were acidified with 1% nitric acid by volume. The correlation coefficients were generally 0.999, or better, and the Relative Standard Deviation of three replicate analyses was always below 5%. The intensity of the background was significantly lower than the intensity of the 1 µg/L standard (about 100 times greater than the background intensity).

Solution phase total Fe concentration was measured by ICP (Perkin Elmer Optima 4000 DV, Atlanta, GA, USA) at 238.294 nm wavelength and Yttrium at 5 mg/L and 371.029 nm was used as an internal standard for calibration.

An Orion-Ross combination glass electrode was used to measure the pH of the solution. The glass electrode was calibrated at 25°C using 4, 7, and 10 pH buffers.

An YSI Inc dissolved oxygen meter was used to measure the DO concentration of the solutions. The electrode was calibrated at 25°C in air saturated water.

2.3 Magnetite nanoparticles

Commercially prepared 20 nm magnetite from Reade Advanced Materials (Reno, NV) was used. In an earlier paper by the authors, Yean et al. (Yean et al. 2005) reported TEM images (not included) and particle characteristics of the 20 nm magnetite showing little size dispersion. From this work the BET surface area was determined to be 60 m^2/g and the nominal particle size calculated using SSA and density was 19.3 nm, as expected (Yean et al. 2005).

2.4 Reactor

The reaction vessel used in this research is a closed container system, Figure S1. It is a one liter glass container with a water jacket to control temperature. The lid is made of stainless steel (316) and has four holes in the lid so that tubing can be connected to the inside of the vessel along with the overhead propeller stirrer/agitator (The Agitator, Arrow Engineering). The connectors are for solution injection and gas sparging, argon gas input, and sampling. PEEK tubing (Western Analytical) was connected to PEEK two or three-way valves (Western Analytical) to keep the system closed from the air. The three-way valves were flushed with nitrogen before and after sampling. The overhead propeller rotated at 120 rpm and changed direction every five seconds.

2.5 Adsorption experiments

Typically, 1 L of 0.01 M THAM was prepared and sparged with Ar gas for 20 min, so a dissolved oxygen concentration of less than 0.3 mg/L (the detection limit of the DO meter) was reached. The stock solution of the species of interest and 100 µg/L of either As(V) or As(III) were added to a sparged solution, and the pH was adjusted to 8.0. The solution was then added to the vessel followed by the quick addition of 0.1 g/L magnetite nanoparticles. The vessel was sealed, and the experiment was conducted under an argon blanket. It took less than 1 min to add the solution, the magnetite, and close the vessel. Since one of the objectives of this research is to develop methods and predictive models to calculate arsenic removal for individual users or for a small treatment plant, most experiments were performed for only 1 or 2 h, and at least two replicates were conducted. The short duration was to ensure that maximum arsenic removal could occur during this time frame. Typically, samples were collected at 5 min, 15 min, 30 min, and 1 h. Samples (10 mL) were taken from the vessel and filtered through a 0.45-µm Nalgene SCFA filter. To ensure that the filter removed the magnetite nanoparticles; several samples were tested to determine the residual iron in solution, which was negligible each time, i.e., less than about 5 µg/L. The pH was checked at the end of each experiment to confirm that negligible pH change had occurred, less than about ±0.05. The solution pH was generally 8.00±0.04 measured at the end of the 1-h experiment.

Near pH 8, aqueous carbonic acid is about 2% of the total carbonate; therefore, simple mass transfer calculations would suggest negligible CO_2 exchange during the experiment (1 h). To check this, two experiments were conducted with 1% CO_2/N_2 mixed gas and 8.2 mM of bicarbonate in

the presence of both As(III) and As(V) at a pH 7.90. There was negligible statistical difference compared to the corresponding argon controls. Thus, argon gas was used throughout the experimentation to avoid using multiple mixed gases. In addition, the presence of the 0.01 M THAM buffer was checked to ensure that there was negligible interference to arsenic adsorption. Two experiments were conducted with 1.6 mM bicarbonate and in the presence and the absence of 0.01 M THAM solution at pH 8.01 ± 0.03 with 100 µg/L arsenate. There was negligible statistical difference between the two experiments, confirming that the THAM buffer did not interfere with arsenic adsorption. Adsorption experiments were also conducted at double and half the hydrogen ion activity, i.e., 7.70 and 8.30 pH and at 20°C and 30°C with little change in observed adsorption (Shipley 2007; Shipley et al. 2009).

Houston tap water was used to measure As(V) adsorption. A tap at Rice University was flushed for 30 min, and 1 L of tap water was spiked with 100 µg/L of arsenic. The spiked tap water was put into the vessel apparatus, and an argon blanket was added. The pH was 7.85. Adsorption experiments were conducted on arsenic contaminated Brownsville, TX groundwater at pH 7.70. The water composition and arsenic speciation are given in an earlier paper by the authors for both Houston tap water and Brownsville groundwater (Shipley et al. 2009).

3 Results and discussion

3.1 Effect of magnetite solid concentration

Arsenate and arsenite adsorption to 0.1 and 0.5 g/L magnetite nanoparticles was conducted, and results were given in an earlier paper by the authors (Shipley et al. 2009). In 1 h, 0.1 g/L magnetite adsorbed 48.5 µg/L of As (V) and 51.2 µg/L of As(III) from an initial concentration of 100 µg/L (expressed as As). Magnetite nanoparticles at 0.5 g/L adsorbed 92.6 µg/L arsenate and 93.9 µg/L arsenite in 1 h. Arsenate and arsenite exhibited similar affinity for the magnetite nanoparticles with an initial arsenic concentration of 100 µg/L. For both As(III) and As(V), the arsenic MCL (10 µg/L As) was reached using 0.5 g/L magnetite nanoparticles. These experiments were repeated several times with a negligible difference between repeat experiments. An adsorption kinetics model has been developed (below) and tested using two drinking water samples.

3.2 Adsorption experiments with species commonly present in water

The effect of calcium, magnesium, fulvic acid (DOM), and sulfate on arsenic adsorption to 0.1 g/L magnetite nano-

particles are summarized in Table 1, where the concentrations of arsenate and arsenite removed from solution at 1.0 h reaction time are listed. Magnetite nanoparticle concentration of 0.1 g/L was used to determine the effect of these species on arsenic adsorption, so the results could be used to develop a sorption kinetics model.

At 1 h, 0.1 g/L of magnetite nanoparticles removed 48.5 µg/L of arsenate and 51.2 µg/L of arsenite, each initially at 100 µg/L in a pH 8.00 solution (Table 1, row 1). These concentrations are used as reference values to quantify the effect of additional species in solution on arsenic removal. Addition of 0.52 mM sulfate had virtually

Table 1 The concentration (µg/L) of arsenate or arsenite adsorbed (Eq. 3) at 1 h with and without the addition of other species to solution with 0.1 g/L magnetite nanoparticles at an initial concentration of 100 µg/L, as As, at pH 8.0

	Species added	As(V) adsorbed in 1h, (µg/L)	As(III) adsorbed in 1h, (µg/L)
1	Reference value (pH 8)	48.5	51.2
2	0.52 mM SO_4^{2-}	48.4	58.4
3	1.04 mM SO_4^{2-}	40.1	44.2
4	2.6 mM SO_4^{2-}	37.7	42.7
5	0.33 mM hardness[a]	39.3	40.7
6	1.32 mM hardness[a]	42.1	43.8
7	0.5 mg/L Fe(II)	55.9	51.2
8	1 mg/L Fe (II)	58.4	59.2
9	5 mg/L fulvic acid	47.0	40.4
10	10 mg/L fulvic acid	41.2	34.1
11	25 mg/L fulvic acid	36.7	28.6
12	0.17 mM SiO_2	35.6	31.2
13	0.42 mM SiO_2	25.0	26.8
14	0.83 mM SiO_2	22.5	26.5
15	1.67 mM SiO_2	25.5	12.3
16	0.16 mM HCO_3^{1-}	44.9	49.3
17	0.82 mM HCO_3^{1-}	37.4	42.9
18	1.64 mM HCO_3^{1-}	34.5	35.6
19	4.1 mM HCO_3^{1-}	28.9	26.2
20	8.2 mM HCO_3^{1-}	25.3	14.4
21	1 µM PO_4^{3-}	45.8	45.8
22	5 µM PO_4^{3-}	27.6	26.3
23	10 µM PO_4^{3-}	22.6	25.1
24	8.2 mM HCO_3^{1-}+1.67 mM SiO_2	15.1	NA[b]
25	0.82 mM HCO_3^{1-}+1.67 mM SiO_2	20.6	NA
26	8.2 mM HCO_3^{1-}+0.17 mM SiO_2	26.2	NA
27	0.82 mM HCO_3^{1-}+0.17 mM SiO_2	37.8	NA

[a] Each at equal mass concentrations of calcium and magnesium expressed in mg/L; e.g., 1.32 mM hardness is 20 mg/L Ca^{2+} (0.50 mM Ca^{2+}) plus 20 mg/L Mg^{2+} (0.82 mM Mg^{2+})

[b] These results were not measured

no effect on arsenate removal (48.5 vs. 48.4 μg/L), whereas 2.6 mM sulfate decreased arsenate removal from 48.5 to 37.7 μg/L. Neutral arsenite adsorption increased slightly at 0.52 mM sulfate and then decreased by about the same amount in 2.6 mM sulfate, which are consistent with that of Vaishya and Gupta (Vaishya and Gupta 2003) on arsenite adsorption. After the addition of 1.32 mM hardness (as 20 mg/L calcium plus 20 mg/L magnesium), 0.1 g/L magnetite removed 42.1 μg/L of arsenate and 43.8 μg/L of arsenite. In summary, the difference in the adsorbed arsenate and arsenite concentrations due to calcium, magnesium, or sulfate at concentrations commonly encountered in potable waters is about 10% or less. The addition of 25 mg/L fulvic acid, as a typical DOM, decreased the arsenate and arsenite removal from 48.5 and 51.2 μg/L to 36.7 and 28.6 μg/L, respectively, in 1 h (Table 1, row 11). The addition of fulvic acid decreased arsenite removal more than arsenate, which is consistent with the results of Grafe et al. (2002).

As expected, phosphate, bicarbonate, and silica at high concentrations had the most significant effect on arsenic adsorption (Table 1). The effect of phosphate on arsenate and arsenite adsorption was negligible when the molar concentration of phosphate (1 μM) was less than the concentration of arsenic (1.3 μM). The arsenate removal decreased to 45.8 μg/L and arsenite to 45.8 μg/L at 1 h, only about a 3% and 5% difference, respectively, in the amount adsorbed compared to the reference values. However, the arsenate removal at 1 h was decreased to 22.6 μg/L and to 25.1 μg/L for arsenite, when the concentration of phosphate was 10 μM. Our results are consistent with other findings (Genc and Tjell 2003; Hongshao and Stanforth 2001; Jain and Loeppert 2000; Su and Puls 2001b; Violante and Pigna 2002), indicating that the presence of phosphate decreased arsenic adsorption, but this work shows that, at common environmentally representative concentrations of phosphate [0.2–2.4 μM (Stumm and Morgan 1996)], phosphate may not be competitive with arsenic adsorption, especially with excess available surface area, as is the case in this work.

With the addition of 0–8.2 mM bicarbonate into solution, the amount of arsenic removed decreased with increasing bicarbonate concentrations (Table 1, rows 16–20). For example, the addition of 8.2 mM bicarbonate decreased the arsenate removal to 25.3 μg/L and arsenite to 14.4 μg/L compared to the reference values. The bicarbonate concentrations used in this paper were similar to the concentrations used by Appelo et al. (2002), Kanel et al. (2005), Su and Puls (2001b), where bicarbonate was observed to decrease arsenic adsorption on ferrihydrite and zero valent iron. The addition of 0.17 mM silica decreased the arsenate removed at 1 h to 35.6 μg/L (Table 1, Row 12–15). When the concentration of silica was ten times greater (1.67 mM), the arsenate removed decreased to 25.5 μg/L

and arsenite to 12.3 μg/L at 1 h. At all the concentrations tested, silica decreased arsenate and arsenite adsorption to magnetite nanoparticles. As observed in this study, Waltham and Eick (2002) observed decreased arsenic adsorption to goethite in the presence of silica, which was believed to be due to decreased surface potential of the goethite upon adsorption of silica creating unfavorable sorption conditions for arsenic.

From the results in Table 1 for individually added species, silica and bicarbonate were chosen for testing together because they are commonly present in drinking water at concentrations that might impact arsenic removal (Table 1, rows 24–27). Based upon the results in Table 1, there does not appear to be a synergistic nor antagonistic effect, at least for bicarbonate plus silica. For example, using the curve fitted coefficients in Table 2 for the effect of 1.67 mM silica and 8.2 mM bicarbonate on arsenic removal and assuming a simple additive inhibition model, it would be predicted that only 12 μg/L of arsenate would be adsorbed at 1 h versus the observed value of 15.1 μg/L (see Table 1, row 24 and modeling section below). This difference might suggest a slight antagonistic effect between silica and bicarbonate, whereby the adsorption of one inhibitor species reduces the inhibition of the other; the combined effect is clearly within expected error of the predicted result using an additive assumption. The assumption seems applicable for our observations and will be tested using naturally occurring groundwater from Texas.

Table 2 The arsenic adsorption rate constants (k), and coefficients of Eqs. 7, 8, and 9 curved fitted with As(III) and As(V) adsorption kinetics data of Table 1 and Fig. 2 and Figure S2 for As(III) and As(V) with 0.1 and 0.5 g/L Fe$_3$O$_4$, various solutions species and iron(III) concentrations

	Units	As(V)	As(III)
K_L	L/g	13.71	15.55
k (0.1 g/L)	h^{-1}	2.00±0.28	2.31±0.20
k (0.5 g/L)	h^{-1}	9.99±1.20	11.59±0.93
$K_{Fe(III)}$	L/mg	1.08±0.08	1.08±0.08
a1 (HCO$_3$)	m^2/mg	0.05±0.01	0.08±0.01
a2 (SiO$_2$)	m^2/mg	0.22±0.11	0.67±0.18
a3 (SO$_4$)	m^2/mg	0.01±0.008	0.01±0.009
a4 (PO$_4$)	m^2/mg	14.10±4.78	24.36±4.95
a5 (DOM)	m^2/mg	0.07±0.01	0.59±0.21
a6 (Ca)	m^2/mg	0.02±0.01	0.06±0.05
a7 (Mg)	m^2/mg	0.02±0.01	0.06±0.05
a8 [Fe(II)]	m^2/mg	-3.30±0.64	-3.12±0.53

The statistical analysis was done using the SolvStat program from E. Billo Excel for Chemist, second edition. K_L values are the linear portion of the Langmuir isotherm for arsenic adsorption to magnetite nanoparticles (Yean et al. 2005)

Much more work is needed to verify that this additive assumption is valid for a wider range of data.

3.3 Iron hydroxide nucleation and subsequent arsenic removal

Ferric chloride is commonly added to water for arsenic removal (Jenne 1979). Most natural waters contain a fraction to a few milligrams per liter of di- or trivalent iron. The impact of increasing the iron concentration on arsenic removal was systematically studied (Fig. 1), and selective data are listed in Table 1. When ferric chloride was added, arsenic removal increased. Adsorption increased because the ferric iron nucleates to form iron(III) hydroxides. This occurs rapidly (within seconds), causing an increase in the amount of surface area available for arsenic adsorption. The presence of 0.5 mg/L ferric iron in solution increased the arsenate and arsenite adsorbed by about 12% compared to when only 0.1 g/L of magnetite nanoparticles was present at 1 h (Fig. 1a, b). As shown in Fig. 1c and d, ferrous iron slightly increases (Table 1, rows 7 and 8) arsenic adsorption, but it does not have such a pronounced effect on arsenic adsorption as does Fe(III). It should be noted that when a low-field handheld magnet was used to remove the magnetite nanoparticles and adsorbed arsenic, the arsenic on the hydrous iron oxide (HFO) remained suspended and was not removed from solution without membrane filtration. The different effects of iron (III) and iron(II) are included in the model in the next section.

These results systematically demonstrate the effect that both cationic and anionic species commonly found in water have on arsenic adsorption to magnetite nanoparticles. Most of the results, except for iron, show that increasing the species concentration decreases the adsorbed arsenic concentration with the most significant effects from high concentrations of phosphate, silica, and bicarbonate. Next, these results are incorporated into a sorption kinetics model to predict arsenic adsorption to magnetite nanoparticles in natural waters.

3.4 Model for prediction of arsenic adsorption to magnetite nanoparticles

A semi-empirical adsorption kinetics model has been developed that describes the observed data and that can be used to model applications of magnetite nanoparticles for arsenic removal from potable water. It is assumed that the adsorption can be described by a first-order process:

$$\frac{d[As]_t}{dt} = -k\left\{[As]_t - [As]_{eq}\right\} \tag{1}$$

$$[As]_t = [As]_{eq} + \left([As]_{in} - [As]_{eq}\right)e^{-kt} \tag{2}$$

Fig. 1 Depicts the amount of arsenic adsorbed when free iron was present in solution along with 0.1 g/L magnetite nanoparticles. **a** The concentration (μg/L) of arsenate adsorbed versus time (h) with 0–5.0 mg/L of ferric iron in solution. **b** The concentration (μg/L) of arsenite adsorbed versus time (h) with 0–5.0 mg/L of ferric iron in solution. **c** The concentration (μg/L) of arsenate adsorbed versus time (h) with 0–1.0 mg/L of ferrous iron in solution. **d** The concentration (μg/L) of arsenite adsorbed versus time (h) with 0–1 mg/L of ferrous iron in solution with a 100-μg/L initial arsenic concentration in 0.01 M THAM buffer solution at pH 8.0. *Errors* bars indicate 5% error in the measurement of arsenic
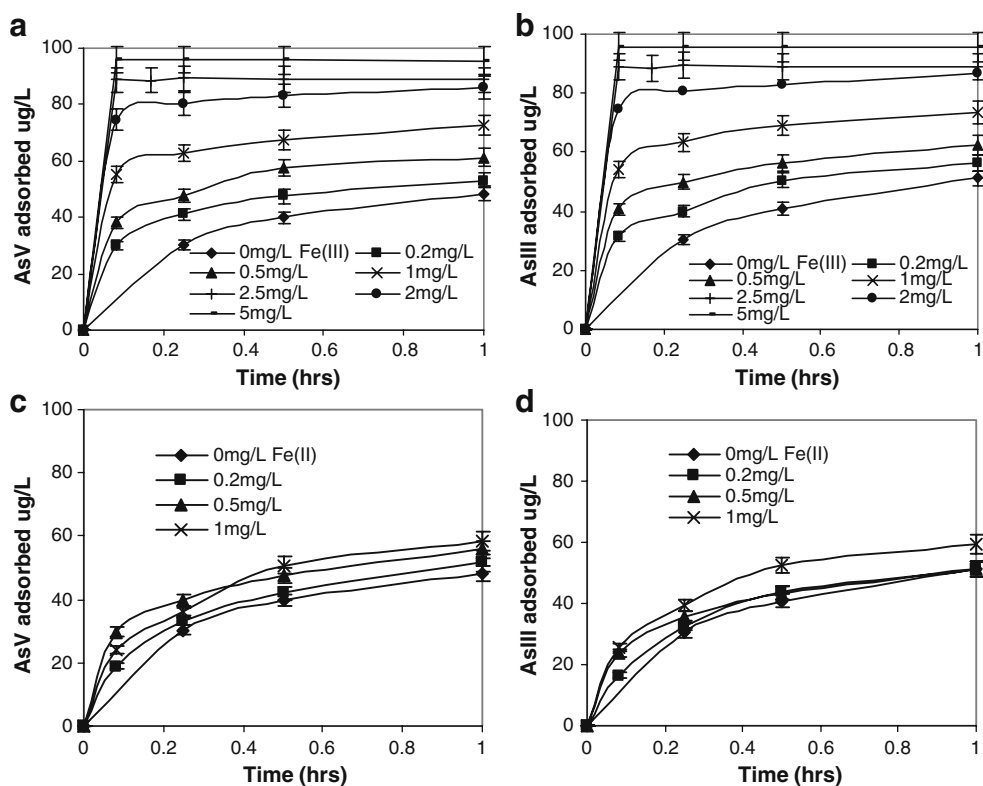
or after multiplying by "−1" and adding $[As]_{in}$ to each side,

$$\left\{[As]_{in}-[As]_t\right\}=[As]_{in}-\left\{[As]_{eq}+\left([As]_{in}-[As]_{eq}\right)e^{-kt}\right\} \tag{3}$$

where $[As]_{in}$, $[As]_t$, and $[As]_{eq}$ are the initial, time t, and equilibrium aqueous concentrations (μg/L) of arsenic, k (h^{-1}) is a first-order rate constant, and $([As]_{in}-[As]_t)$ in Eq. 3 is the concentration of arsenic adsorbed (arsenic concentration removed from solution) in Table 1. The $[As]_{eq}$ can be calculated from a mass balance condition (Eq. 4) and the adsorption isotherm (Eq. 5):

$$[As]_{in}=[As]_{eq}+q_{As,eq}r_{sw} \tag{4}$$

where $q_{As,eq}$ is the arsenic adsorption at equilibrium (μg/g), and r_{sw} is the magnetite solid mass/solution volume ratio (g/L). A Langmuir adsorption isotherm has been found to fit the arsenic adsorption to magnetite nanoparticles well (Yavuz et al. 2006; Yean et al. 2005). All of the experiments herein are in the linear region of the Langmuir isotherm and can be expressed as:

$$q_{As,eq}\cong K_L[As]_{eq} \tag{5}$$

with K_L (L/g) as the linear slope (see Figure S2). Substituting Eq. 5 into 4 and rearranging:

$$[As]_{eq}=\frac{[As]_{in}}{(1+K_Lr_{sw})} \tag{6}$$

Finally, substituting Eq. 5 into 2 and simplifying (Shipley et al. 2009):

$$[As]_t=\left(\frac{[As]_{in}}{1+K_Lr_{sw}}\right)\left(1+K_Lr_{sw}e^{-kt}\right) \tag{7}$$

The rate constant, k(h^{-1}), can be expressed as the product of the magnetite concentration times the specific surface area times a mass transfer-type rate constant, k_m(m s^{-1}). For example, with $k=2$ h^{-1}, $r_{sw}=0.1$ g L^{-1}, and SSA$=60$ m^2 g^{-1}

the mass transfer constant, $k_m=k\cdot(r_{sw}\times SSA)^{-1}=3.33\times10^{-4}$ m h^{-1}, and since k in Table 2 is directly proportional to r_{sw}, the value of k_m is system independent.

Two additional modifications to Eq. 7 are needed to model the removal of arsenic from typical drinking waters, the effect of iron(III), and the effect of other common species in the water. The effect of added ferric ions, commonly added as ferric chloride, has been systematically studied for both As(III) and As(V), see Fig. 1. When increasing concentrations of ferric chloride are added to solutions containing either As(III) or As(V) and 0.1 g/L of magnetite nanoparticles, the solution arsenic concentration initially decreases rapidly, within a minute, and then the remaining arsenic in solution independently adsorbs to the magnetite nanoparticles. All the data in Fig. 1 for both As (III) and As(V) can be modeled using Eq. 7 by assuming that the $[As]_{in}$ is reduced at the beginning, as follows:

$$[As]_{in,Fe(III)Added}=[As]_{in}/\left\{1+K_{Fe(III)}\times TotFe(III)\right\} \tag{8}$$

with TotFe(III) expressed as milligram per liter; the value of $K_{Fe(III)}$ was found to be 1.08 (±0.08) L/mg ($r=0.98$, Table 2). This value of $K_{Fe(III)}$ is consistent with Visual Minteq modeling. Using the default parameters for HFO in Visual Minteq 2.52 and assuming that all iron (III) added is converted to HFO, 1 mg/L of TotFe(III) will produce about 1.61 mg/L of HFO at pH 8. Using Visual Minteq, this amount of HFO at pH 8 is calculated to adsorb 61% and 85% of As(III) and As(V), respectively, versus 64% calculated using Eq. 8 for both As(III) and As(V). Small variations in the assumed properties of the HFO, such as site density or specific surface area (Dzombak and Morel 1990), would match the observed effect of ferric ions, seen in Fig. 1.

The effect of additional components in the water on the adsorption of arsenic is summarized in Table 1. It is proposed that the data in Table 1 can be modeled by assuming a simple competitive inhibition model, which is additive in the denominator (Fig. 2), i.e., inhibition can be thought of as removing available magnetite nanoparticle surface sites for arsenic attachment (Dayong et al. 2008;

Fig. 2 Plot of measured arsenic adsorption in the presence of species versus the calculated arsenic adsorption by Eq. 10 arsenate (**a**) arsenite (**b**)
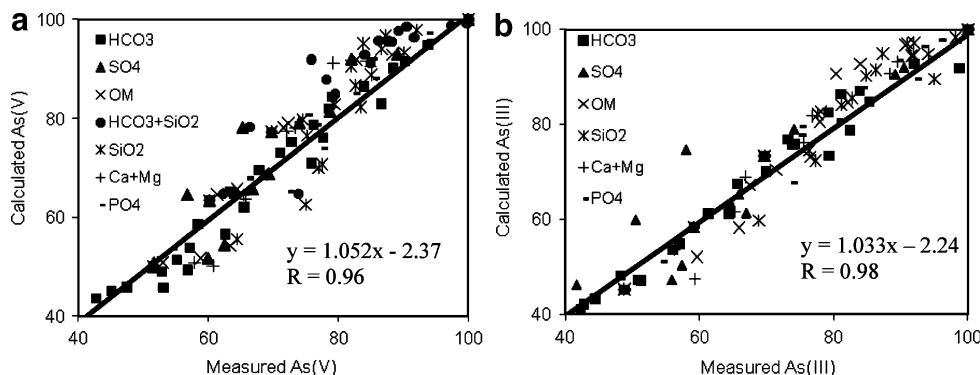
Krupka 1983). This can be done by dividing the rate constant, k, in Eq. 7 by a term, C as follows:

$$C = 1 + \left(\sum a_i [X_i] \right) (r_{sw} \times SSA) - 1 \tag{9}$$

where $[X_i]$ is the concentration of the ith species (mg/L), a_i (m²/mg) is a curve-fitted constant for each species, listed in Table 2. Dividing each concentration, $[X_i]$, by ($r_{sw} \times SSA$) normalizes the inhibition for total surface area so that the a_i terms can be used for other solid/solution ratios and particle sizes.

Finally, substituting Eqs. 8 and 9 into 7 and simplifying:

$$\frac{[As]_t}{[As]_{in}} = \left(\frac{1}{1 + K_{Fe}[TotFe_{III}]} \right) \left(\frac{1}{1 + K_L r_{sw}} \right) \left(1 + K_L r_{sw} e^{-kt/C} \right) \tag{10}$$

gives the overall sorption kinetics model. All of the experimental adsorption kinetics data used in this research to develop the results in Table 1 for both As(III) and As(V) were modeled using Eq. 10 (see Fig. 3). Including the effect of Fe(III) in Fig. 1 would not significantly alter the agreement between predicted and measured arsenic values. The good agreement between the measured and calculated concentrations of arsenic suggests the overall robustness of the model to represent the impact of aquatic species on arsenic adsorption to magnetite.

3.5 Model prediction of arsenic adsorption in arsenic contaminated tap water and groundwater

Arsenic adsorption experiments to magnetite nanoparticles were conducted with spiked Houston tap water and arsenic contaminated groundwater from Brownsville, TX (Fig. 3). For spiked tap water, Fig. 3a shows the measured and the predicted arsenate adsorbed from solution. The initial concentration of arsenate in solution was 100 and 0.5 g/L of magnetite nanoparticles removed 83% of the arsenate from solution within an hour. Calculated versus measured arsenic concentration has a correlation coefficient, $r=0.97$.

The Brownsville, TX groundwater contains high concentrations of several species such as bicarbonate and silica. Preliminary calculations suggested that 0.5 g/L magnetite nanoparticles would remove the arsenic from the groundwater, which gave a concentration less than 10 μg/L (the EPA MCL) in less than 10 min. The presence of 7.60 mM bicarbonate, 0.60 mM silica, and other high concentrations of species did not prevent the removal of arsenic by the magnetite nanoparticles, and negligible iron residuals were detected after filtration. Figure 3b shows the measured and the predicted arsenic adsorbed from solution. Our model slightly overpredicts what occurred experimentally (Fig. 3a, b). The overprediction by our model may be due to the assumption that ferric iron concentration in the model is the total iron concentration measured. In fact, it is more likely that the total iron consisted of both ferrous and ferric iron in which the ferrous iron would not significantly contribute to increasing arsenic adsorption unless high concentration (>1 mg/L) were present in solution (Fig. 1). Still, the predicted results by the model fit the measured results reasonably well with a correlation coefficient, $r=0.99$.

4 Conclusion

These results demonstrate the ability of the magnetite nanoparticles to remove arsenic from potable waters. The increased surface area of the nanoparticles along with the low iron residuals and ease of separation offers a potential method of treatment for individual household use. Based on
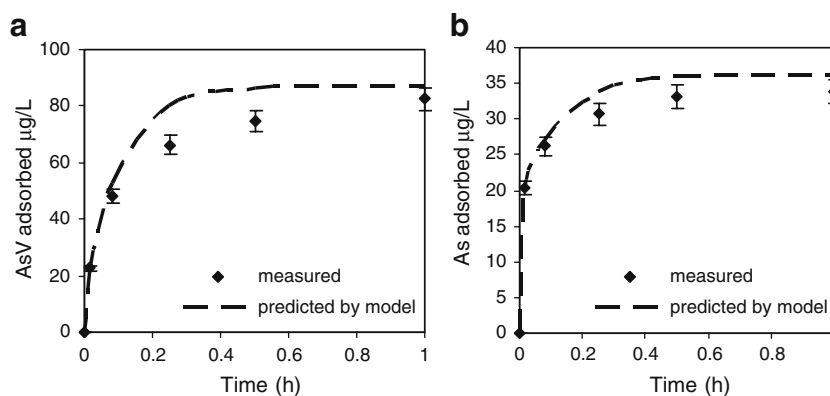

Fig. 3 Plot of arsenate adsorbed (μg/L, as As) versus time (h) for 100 μg/L spiked Houston tap water with 0.5 g/L magnetite nanoparticles (**a**). Plot of arsenic adsorbed (μg/L, as As) versus time (h) for arsenic contaminated Brownsville, TX well water with 0.5 g/L magnetite nanoparticles (**b**). The *symbols* are the experimental data, and the *dashed line* is the fitted value from Eq. 10 and Table 2. *Errors bars* indicate 5% error in the measurement of arsenic

our observations, the developed model accurately predicts arsenic adsorption to magnetite nanoparticles and the impact of common species present in drinking water. This work might be applied to other contaminants such as heavy metals and used for treatment design, though much more work is needed to make these results applicable for wider ranges of data.

References

Anderson LCD, Bruland KW (1991) Biogeochemistry of arsenic in natural waters: the importance of methylated species. Environ Sci Technol 25:420–427

Appelo CA, Van Der Weiden MJJ, Tournassat C, Charlet L (2002) Surface complexation of ferrous iron and carbonate on ferrihydrite and the mobilization of arsenic. Environ Sci Technol 36:3096–3103

Arai Y, Sparks DL, Davis JA (2004) Effects of dissolved carbonate on arsenate adsorption and surface speciation at the hematite–water interface. Environ Sci Technol 38:817–824

Banfield JF, Navrotsky A (2003) Nanoparticles and the environment. Reviews in mineralogy and geochemistry. Geochim Cosmochim Acta 67:1753

Coker VS, Gault AG, Pearce CI, Vanderlann G, Telling ND, Charnock JM, Polya DA, Lloyd JR (2006) XAS and XMCD evidence for species-dependent partitioning of arsenic during microbial reduction of ferrihydrite to magnetite. Environ Sci Technol 40:7745–7750

Cornell RM, Schwertmann U (1996) The iron oxides: structure, properties, reactions, occurrence and use. Weinheim, New York 573 pp

Dayong S, Wang Y, Guo Y, Wang J, Zhou H, Zhou Y-H, Li Z-S, JP F (2008) Mechanism of CYP2C9 inhibition by flavones and flavonols. Drug Metab Dispos 37:629–634

Dixit S, Hering JG (2003) Comparison of arsenic(V) and arsenic (III) sorption onton iron oxide minerals: implications for arsenic mobility. Environ Sci Technol 37:4182–4189

Dzombak DA, Morel FM (1990) Surface complexation modeling: hydrous ferric oxide. Wiley, New York

Frankenberger WT (ed) (2002) Environmental chemistry of arsenic. Soils, plants, and the environment. Marcel Dekker, New York, 391 pp

Genc H, Tjell JC (2003) Effects of phosphate, silicate, sulphate, and bicarbonate on arsenate removal using activated seawater neutralized red mud. J Phys IV France 107:537–540

Gimenez J, Martınez M, Jd P, Rovira M, Duroc L (2007) Arsenic sorption onto natural hematite, magnetite, and goethite. J Hazard Mater 141:575–580

Grafe M, Eick M, Grossl P, Saunders A (2002) Adsorption of arsenate and arsenite on ferrihydrite in the presence and absence of dissolved organic matter. J Environ Qual 31:1115–1123

HACH (2007) HACH water analysis handbook procedures. HACH, Loveland

Hering JG, Chen P-Y, Wilkie JA, Elimelech M (1997) Arsenic removal from drinking water during coagulation. J Environ Eng 123:800–807

Hongshao Z, Stanforth R (2001) Competitive adsorption of phosphate and arsenate on goethite. Environ Sci Technol 35:4753–4757

Jain A, Loeppert RH (2000) Effect of competing anions on the adsorption of arsenate and arsenite by ferrihydrite. J Environ Qual 29:1423–1430

Jenne EA (1979) Chemical modeling in aqueous systems. ACS Symposium. American Chemical Society, Washington

Kanel SR, Manning B, Charlet L, Choi H (2005) Removal of Arsenic (III) from groundwater by nanoscale zero-valent iron. Environ Sci Technol 39:1291–1298

Krupka RM (1983) The kinetics of transport inhibition by noncompetitive inhibitors. J Membr Biol 74:175–182

Meng X, Bang S, Korfiatis GP (2000) Effects of silicate, sulfate, and carbonate on arsenic removal by ferric chloride. Water Res 34:1255–1261

O'Day PA, Vlassopoulous D, Meng X, Benning LG (ed) (2005) Advances in arsenic research. ACS Symposium. Oxford University Press, USA, 433 pp

Ohe K, Tagai Y, Nakamura S, Oshima T, Baba Y (2005) Adsorption behavior of As(III) and As(V) using magnetite. J Chem Eng Jpn 38:671–676

Pierce ML, Moore CB (1982) Adsorption of arsenite and arsenate on amorphous iron hydroxide. Water Res 16:1247

Raven KP, Jain A, Loeppert RH (1998) Arsenite and arsenate adsorption on ferrihydrite: kinetics, equilibrium, and adsorption envelopes. Environ Sci Technol 32:344

Rusanov AI (2005) Surface thermodynamics revisited. Surf Sci Rep 58:111

Shipley HJ (2007) Magnetite nanoparticles for removal of arsenic from drinking water. Rice University, Houston, 147 pp

Shipley HJ, Yean S, Kan AT, Tomson MB (2009) Effect of solid concentration, pH, IS, and temperature on arsenic adsorption. Environ Toxicol Chem 28:509–515

Smedley PL, Kinniburgh DG (2002) A review of the source, behavior, and distribution of arsenic in natural waters. Appl Geochem 17:517–568

Stumm W, Morgan JJ (1996) Aquatic chemistry, 3rd edn, vol 60. Wiley, New York

Su C, Puls RW (2001a) Arsenate and arsenite removal by zerovalent iron: kinetics, redox transformation, and implications for in situ groundwater remediation. Environ Sci Technol 35:1487–1492

Su CM, Puls RW (2001b) Arsenate and arsenite removal by zerovalent iron: effects of phosphate, silicate, carbonate, borate, sulfate, chromate, molybdate, and nitrate relative to chloride. Environ Sci Technol 35:4562–4568

Vaishya R, Gupta S (2003) Arsenic removal from groundwater by iron impregnated sand. J Environ Eng 129:89–92

Violante A, Pigna M (2002) Competitive sorption of arsenate and phosphate on different clay minerals and soils. Soil Sci Soc Am J 66:1788–1796

Waltham C, Eick M (2002) Kinetics of arsenic adsorption on goethite in the presence of sorbed silicic acid. Soil Sci Soc Am J 66:818–825

Waychunas GA, Davis JA, Fuller CC (1995) Geometry of sorbed arsenate on ferrihydrite and crystalline FeOOH: re-evaluation of EXAFS results and topological factors in predicting sorbate geometry, and evidence for monodentate complexes. Geochim Cosmochim Acta 59:3655

World Health Organization (2001) Arsenic in the drinking water. Fact Sheet 210. WHO Media Center, Geneva

Yalcin S, Le XC (2001) Speciation of arsenic using solid phase extraction cartridges. J Environ Monit 3:81–85

Yavuz CT, Mayo JT, Yu WW, Prakash A, Falkner J, Yean S, Cong L, Shipley HJ, Kan AT, Tomson MB, Natelson D, Colvin VL (2006) Low-field magnetic separation of monodisperse Fe_3O_4 nanocrystals. Science 314:964–967

Yean S, Cong L, Yavuz CT, Mayo JT, Yu WW, Kan AT, Colvin VL, Tomson MB (2005) Effect of magnetic particle size on adsorption and desorption of arsenite and arsenate. J Mater Res 20:3255–3264